Visible/NIR imaging spectroscopy for assessing quality and safety of agro-foods

Yud-Ren Chen and Moon S. Kim

Instrumentation and Sensing Laboratory, Henry A. Wallace Beltsville Agricultural Research Center, Agricultural Research Service, United States Department of Agriculture, Beltsville, MD 20705-2350 USA

Introduction

Near-infrared (NIR) technology has been successfully used for food quality analysis during the past three decades. A review of the applications of NIR spectroscopy to agricultural products was recently given by Shenk and Workman.[1] The advantages of near-infrared spectroscopy for quality assessment are that it is a rapid and non-invasive technique, samples do not require dilution, and the procedure is simple. However, it acquires gross averages of the quality of the material. In general, most applications require homogenized samples. Recently, research has been conducted at the Instrumentation and Sensing Laboratory (ISL) to acquire NIR spectra of single or bulk intact kernels of wheats for classification or for prediction purposes.[2,3]

In the last decade at ISL extensive research has also been conducted to apply visible and near-infrared (Vis/NIR) technology for on-line safety inspection of poultry carcasses.[4-7] But the application is limited to sensing over a large surface area of the products. The technology is not suitable for detection of inhomogeneity or localized diseases or defects of agro-foods.

On the other hand, imaging techniques have been investigated as an inspection tool for assessing the quality and safety of a variety of agricultural food products. Besides size and shape information, imaging also provides information on the texture and color distribution of the sample surface which may be indicative of certain inferiorities in quality or abnormalities, such as diseases or defects.[8-13] The application of imaging systems for the detection of diseases and defects, however, has not been fully exploited, because complicated and intensive image processing procedures are required for image analysis. Image processing algorithms are often task specific.

In order to take advantage of differences in the responses of agro-foods to radiation at different wavebands in the visible and near-infrared region for improvement of the detection power of imaging systems, multiple spectral bands are used for detection of defects and diseases on the surface of agro-foods.[14-19] However, no easy methods are available for choosing the optimal filter sets for multispectral imaging systems that are suitable for any given food or agricultural product. In fact, the determination of appropriate filters to use for each agro-product has been mostly experimental.

Imaging spectroscopic techniques

Imaging spectroscopy, commonly called hyperspectral imaging (HSI), has recently emerged as a powerful technique in earth remote sensing.[20] This technique combines the features of imaging and spectroscopy to acquire both spatial and spectral information from an object simultaneously. The technique yields more useful information than other imaging techniques because each pixel on the image surface possesses a spectral signature of the object at that pixel. This greatly enhances its

Near Infrared Spectroscopy: Proceedings of the 11th International Conference.

capabilities to identify materials and detect subtle and/or minor features in an object. Applications range from precision agriculture applications, such as detection of plant stress or crop infestation, to medical applications, and agricultural product quality and safety sensing.

The major applications of hyperspectral imaging with respect to food safety and quality are either to detect the existence of abnormal or blemished products, or to classify abnormal or blemished parts from the wholesome parts of the products, based on their spectral signatures. For example, contamination detection involves searching the pixels of the HSI data cube that indicate the presence of specific material or contaminants. It can look for pixel content significantly different from the spectral content of the local background. This is the case of detection. On the other hand, pixels of the HIS data cube can be sorted into different classes, a case of classification.

Hyperspectral image data acquisition

Two image cube acquisition methods are suitable for sensing agricultural products for safety and quality applications. The first approach is to sequentially capture a series of narrow-band spectral images to produce a three-dimensional image cube. This can be accomplished by using multiple bandpass filters, liquid-crystal tunable filters, or acousto-optic tunable filters for acquisition of hyperspectral images.

The second approach is a pushbroom method by which a line of spatial information with a full spectral range per spatial pixel is captured sequentially to complete a volume of spatial-spectral data. The fact that CCD detectors have two-dimensional arrays and a spectrograph allows simultaneous recording of a line of spatial and a multiple of spectral information. The advantage of this type of system is that sample size in one of the spatial directions is not limited by the size of CCD as compared to the first approach.

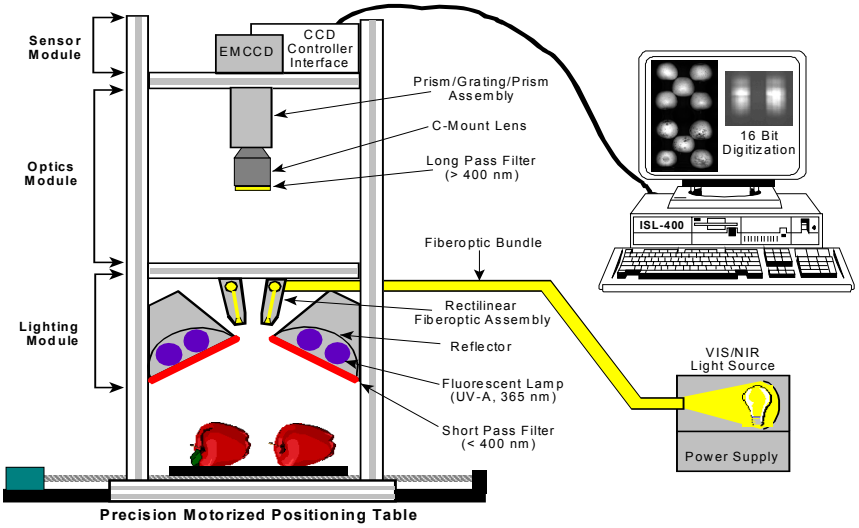

Figure 1. ISL hyperspectral imaging system for food safety and quality study.

Figure 1 is a schematic diagram of the hyperspectral imaging system that is currently utilized at the Instrumentation and Sensing Laboratory (ISL) for capturing spectral data of various food

products for the possible presence of contamination. It consists of a CCD camera system, equipped with an imaging spectrograph. The image spectrograph has a fixed-size internal slit to define the field of view (FOV) for the spatial line and a prism/grating/prism system for the separation of the spectra along the spatial line. The image acquisition and recording are performed with a PC using in-house imaging software operating in the windows environment.

The system is equipped with two independent illumination sources for reflectance and fluorescence measurements. The light source for reflectance measurements consists of halogen lamps powered with regulated DC voltage power supplies. The light is transmitted through optical fibers to a line light to illuminate target areas. For fluorescence measurements, two fluorescent lamp assemblies provide a near uniform UV-A (365 nm) excitation to the sample area. Short-pass filters placed in front of the lamp housing are used to prevent transmittance of radiation greater than approximately 400 nm to eliminate potential spectral contamination by pseudo-fluorescence. A precision positioning table transports sample materials through the FOV line in transverse direction while the stationary imaging system acquires data via line-by-line scans. Sample materials are placed on a tray painted with non-fluorescent, flat black paint to minimize background scattering. Measurements are conducted without room light. A more complete description of the system and details of spectral and spatial calibrations can be found in Kim, et al.[21, 22]

Hyperspectral imaging data cube

Hyperspectral imaging yields a 3-D (dimensional) array or "cube" of data, stacking single-band images along a spectral axis. Each data value represents the intensity of a pixel and it can be denoted by $\mathbf{I}(u,v,\lambda)$, where u and v are spatial dimensions with u=1,2,..,M, v=1,2,..,N, and λ is the spectral dimension that has a discrete value from λ_1 to λ_k.

For a fixed λ_k, $\mathbf{I}_k(u,v)$ represents the *k*-th spectral band image, that is, spatial information. If u and v are fixed, then $I_{u,v}(\lambda)$ represents the spectrum at that pixel, i.e., spectral information. Images from two adjacent bands (λ_j and λ_{j+1}) can have a high degree of similarity, while images from distant bands can be much less similar and may have independent information.

Dimensionality reduction

In general, HSI systems are built with a large number of narrow spectral bands so that they will provide suitable data for a broad spectrum of applications. The sensor system oversamples the spectral images to ensure that any narrow band features are adequately represented. Typical hyperspectral images contain hundreds to thousands of samples. However, it has been shown that high dimensional spaces are mostly empty and that a smaller subspace will contain the significant structure needed for a given classification problem.[23] Such applications that reduce the image dimensionality to a lower-dimensional space are called data representations.

Spatial and spectral dimensionalities can be reduced using principal component analysis, Fourier transformation, or wavelet transformation. Most dimensionality reduction for image representation is done in the spectral dimension, using principal component analysis (PCA). PCA retains most data variance, and eliminates variance due to noise.

PCA approximates the spectral vector $\mathbf{x}$ with a linear combination of a set of (orthonormal, uncorrelated) eigenvectors, $\Phi_P = [\phi_1, \phi_2, \phi_3, \ldots \phi_P]$, also known as factors:

$$\mathbf{z} \cong {}_P{}^T y_P \tag{1}$$

where $\mathbf{z}$ is the approximation of $\mathbf{x}$, the elements, y_p, of y_P are the projections of the vector $\mathbf{x}$ onto the basis vector, ϕ_P, and superscript, T, means transpose of the matrix. To find Φ_P is to minimize

the mean square error between **x** and the approximation **z** obtained from Equation 1, or Φ_P is selected so that expected value of $[(\mathbf{x} - \Phi_P^T y_P)^2]$ is minimized.

The first eigenvector, ϕ_1 (also called first factor) accounts the largest possible variance of reflectance in the samples (largest eigenvalue of the covariance matrix of the sample spectra). Each successive principal component or factor accounts for the largest possible amount of the remaining variance. Each spectrum can be adequately represented by a few factors in factor space. In this way, the K dimension of the spectra in wavelength space can be transformed into a vector space with P dimensions spanned by P factors, where $P \leq K$.

Figure 2 shows that the 4th principal component image of 6 apples, of which 3 are wholesome and 3 have blemishes.

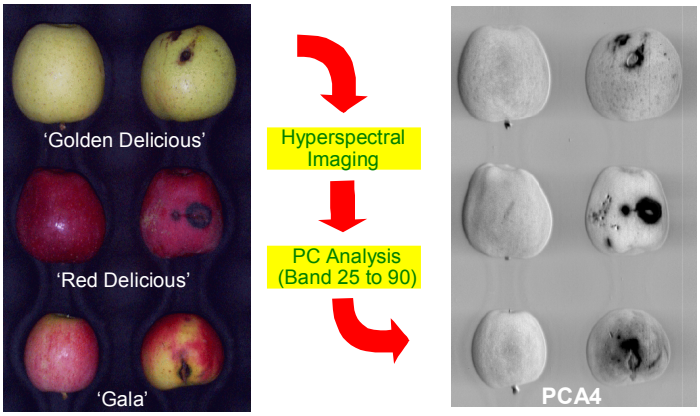

Figure 2. The fourth principal component image of apples with different defects. First column apples are wholesome, and the second column apples are with blemishes.

It shows that the blemishes on the apple surface could be enhanced in some PCA images. However, without visual review of all the PCA images, it is difficult to determine which PCA image would yield the best results. Also, the standard PCA method may not always yield good separation of blemishes from the wholesome parts as shown in Figure 2. Standard PCA is effective in data representation, which only requires the first major principal components with high eigenvalues. But effective discrimination may be found in the PCA images with low eigenvalues. This is because the very first components in general extract the commonalities in the features that best represent the images. However, subtle differentiation requires some components with lower eigenvalues for successful classification.

Feature extraction and selection

An important operation of hyperspectral image processing is to eliminate the redundancy in the spectral and spatial sample data while preserving the essential features needed for discrimination. Therefore, it is important to find a means for finding the most appropriate subspace as soon as the classes to be separated have been defined. Dimensionality reduction should preserve the information of interest for down stream analyses. The high dimensional space is reduced to a lower dimensional feature space. Although principal component analysis can reduce dimensionality of the

imaging data, it typically does not provide the best features for discrimination. In seeking the optimal subspace, the primary axis of the transformation should be oriented such that the classes have the maximum separability between their means on the new axis, while at the same time they should appear as small as possible within their individual spreads.

Fisher's linear discriminate analysis technique is often used for class-based feature extraction. The task is to find new axes such that the ratio between the between-class variance and average of within-class variance is maximized, that is, to maximize the separation of the two class centers, and minimize the spreads of the individual classes.

Figure 3 shows examples for separating wholesome and chilling-injured cucumbers. Two features are used: the y-coordinate is the feature of mean image intensity and the x-coordinate is the variance of image intensity. It clearly shows that the class-based Fisher's linear discriminate function can separate chilling-injured cucumbers, while dimensional reduction principal component failed to separate them.

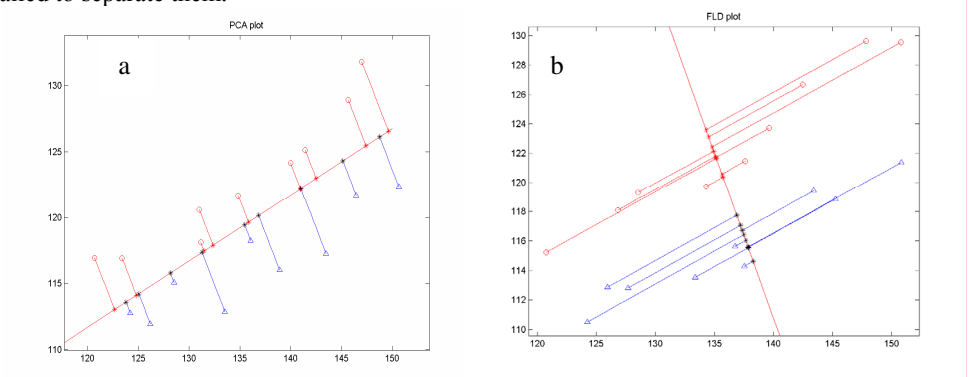

Figure 3. Shows the data are projected onto the principal component in the feature space using covariance matrix of the sample image (a), and the projection are onto the principal component which maximizes the separation of the class center and minimize the variance of each class (b). x-coordinate– feature 1; y-coordinate– feature 2, 'o' – wholesome cucumbers; and "Δ"– chilling injured cucumbers

The Fisher linear discriminant is well suited for separating image data for different objects or classes by reducing intra-class variations and increase inter-class separation. But it does not attempt to be a good representation of the original data set. It is also only good for the classification when each class has only one cluster. It could not classify well the classes with multiple clusters. In order to address these issues, Talukder and Casasent[24] recently proposed generalized linear and non-linear feature extraction methods that simultaneous represent and classify classes with multiple clusters.

Procedure for classifying classes in hyperspectral images

Before extracting and selecting features and establishing a model for discrimination using a training set, digital image processing is generally performed with a computer to manipulate information within an image to make it useful. Image processing may include background elimination, segmentation, region of interest selection, and other image enhancement procedures such as morphological operations and filtering to correct inconsistencies in the acquired images caused by nonuniform illumination.

To separate two or multiple classes of spectra or features (vectors), a discriminant function g(x) is often formed, where x is a feature vector. With *m* classes $\{g_1(x), g_2(x), \ldots, g_m(x)\}$ and ω_i

denotes the i-th class, if $g_i(x)$ is greater than or equals to $g_j(x)$ for all $j = 1, \ldots, m$, then feature vector x belongs to class ω_i. For example, $g_i(x)$ can be directly related to the class conditional density function for class ω_i for all classes. If the 2nd order statistics can be adequately applied to the data set, a simple discriminate function g(x) can be the minimum distance to the class means if class variance in all features is unity and the features are all uncorrelated to one another. When all classes have the same co-variance matrix and correlation structure, the discriminant function becomes $g_i(\mathbf{x}) = -(\mathbf{x} - \mu_i)^T S^{-1} (\mathbf{x} - \mu_i)$, where μ_i are the class mean and S is the co-variance matrix of the sample data. For nonequal variances in the classes, a Quadratic (Gaussian) classifier, $g_i(\mathbf{x}) = -(1/2) \ln S_i - (1/2) [(\mathbf{x} - \mu_i)^T S_i^{-1} (\mathbf{x} - \mu_i)]$, is often used, where S_i is the co-variance matrix of class ω_i.

The aforementioned classifiers are optimal when the data have Gaussian distribution. These classifiers extract information from the second-order correlations in the data. It implicitly assumes that probability density functions of the data are unimodal, and are symmetrically distributed about the means. Higher order statistics or non-parametric techniques such as artificial neural networks are often required for achieving effective discrimination of agricultural products for safety and quality assessment.

An artificial neural network (ANN), which is a non-parametric scheme, learns by example to recognize patterns in data. It seeks out patterns in data sets that relate input variables to output states. They learn these patterns and develop the ability to correctly classify new data sets based on the learned patterns. A network receives a number of inputs (feature vector) and produces an output, the network's classification.[25]

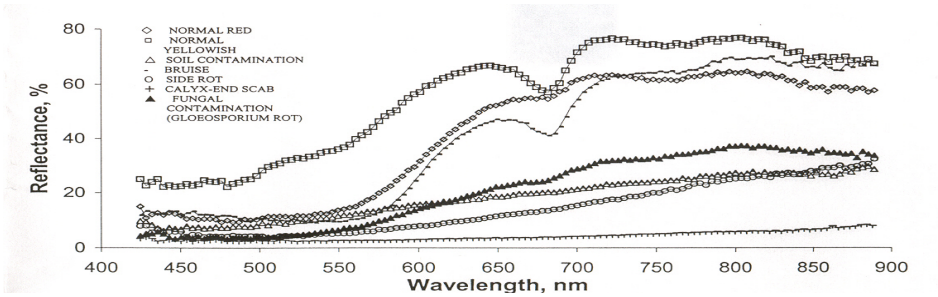

Figure 4. Typical spectra extracted from the hyperspectral image data for the uncontaminated and contaminated surfaces of red delicious apples.

Selection of wavebands for real-time multispectral imaging system

ISL has been actively conducting research to develop methodology for optimal feature selection from the hyperspectral imaging data, and for selecting optimal wavelengths for multispectral imaging systems for rapid on-line implementation.

In a study, 3 wavelengths were selected from hyperspectral imaging data and were implemented into a common aperture multispectral imaging system for detection of blemishes, including side rots, bruises, flyspecks, scabs and molds, black poxes, and fungal and soil contaminations, on apples. The advantage of common aperture multispectral imaging is that it can simultaneously acquire multiple spectral images. It facilitates accurate processing of multiple images of different spectral bands, such as subtractions and additions. And most of all, it can run in real-time.

Figure 4 illustrates typical reflectance spectra extracted from hyperspectral image data for the uncontaminated and contaminated surfaces of red delicious apples. In general, uncontaminated apple surfaces showed higher reflectance in the Vis (> 600 nm) and NIR regions compared to the defective or contaminated surfaces, except for bruised spots, which have higher reflectance. Areas with scabs exhibited the lowest reflectance. There was a very distinct absorption feature in the red region of the spectrum with maximum absorption centered at around 680 nm. This absorption was due to the presence of chlorophyll *a* molecules. The contaminated spots lacked the chlorophyll *a* absorption features, except for bruised areas. Low reflectance characteristics observed in the region from approximately 450 nm to 550 nm for uncontaminated apples were the manifestation of strong absorption by the constituent pigments such as chlorophyll *b* and carotenoids.

We can differentiate between contaminated and uncontaminated apples and discern where the contaminated portions are; however, this cannot be easily done using a single wavelength image. Due to the non-flat shape of apples, reflectance measurements vary greatly across apples from the center to edges. This variation masks the differences that might be seen for either contaminated or uncontaminated conditions. A modified second difference method, with different gaps (asymmetric) for the lower and upper wavelengths from the center wavelength, was defined.[26]

$$\Delta^2 S(\lambda_n, g_1, g_2) = [g_1 S(\lambda_n - g_1) - (g_1+g_2) S(\lambda_n) + g_2 S(\lambda_n + g_2)] / (g_1+g_2) \quad (2)$$

where $\Delta^2 S(\lambda_n, g_1, g_2)$ is the asymmetric second difference image of $S(\lambda_n)$ with gaps, g_1 and g_2, where g_1 is not equal to g_2.

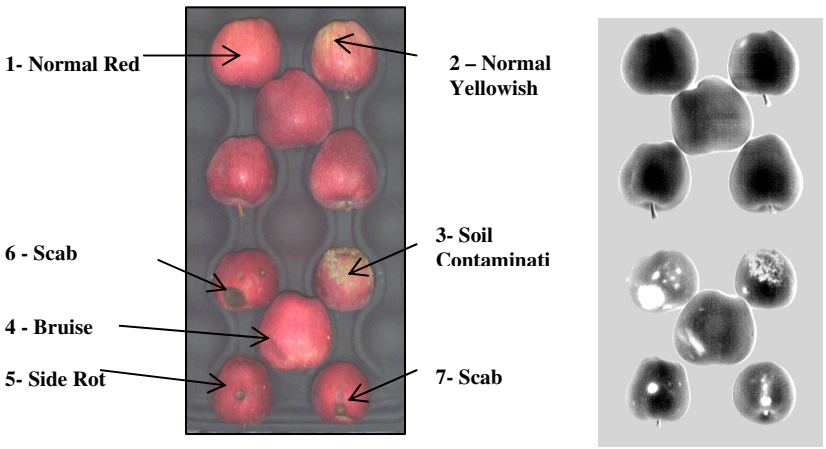

Figure 5. Color(left) and asymmetric second difference (right) images with three bands centered at 720 nm, with g_1 = 40 nm and g_2= 145 nm.

Figure 5 shows colour (left) image and asymmetric second difference (right) image with the centre band at 720 nm, g_1 = 40 nm, and g_2= 145 nm. Various white spots within the apples depict the defects and contamination on apples. All the uncontaminated apples showed no defects or contamination except the one apple positioned at the upper-right corner. The white spots shown in Figure 5 for the uncontaminated apple image is believed to be an actual tiny bruised spot. More detail is provided in Mehl, et al.[26]

We have also investigated other apple cultivars including Gala, Fuji, and Golden Delicious (data not shown) and obtained similar results. The above three spectral bands are being implemented in a 3-channel common aperture imaging system for on-line inspection of apple cultivars for diseases, defects, and soil contamination.

In an attempt to find 2 to 4 wavelengths that could potentially be used in a multispectral imaging system for on-line inspection of fecal contamination on apples, first 6 principal component images were extracted from hyperspectral reflectance image data of 4 fecal-contaminated cultivars of apples, including Red Delicious, Gala, Fuji and Golden Delicious. The 6 principal component images were evaluated visually to determine which PC image has the least variation in uncontaminated sample surfaces and the largest contrast between contaminated spots and sample surfaces. Based on visual assessment, the PC-3 images for all cultivars appeared to provide the best discrimination between the feces treated spots and uncontaminated apple surfaces regardless of apple colorations. From the PC-3 image, 2 to 3 wavelengths with highest absolute (local maxima) weighing coefficients were then selected as the dominant wavelengths. Principal components (images) using only the selected dominant wavelengths (multispectral images) were re-calculated. Results showed that contamination could be identified using either 3 wavelengths in the green (549.5-560.6 nm) , red (678.2-703.9 nm), and NIR (851 nm) regions, or 2 wavelengths (748 and 851 nm) at the extremes of the NIR region under study. However, using 2 NIR wavelengths was found to be less sensitive to variations in apple coloration. Detail of the study can be found in Kim et al.[27]

The hyperspectral imaging system was further used to obtain fluorescence images of apples of the same four varieties, with an excitation wavelength at 365 nm. Using the same procedure for identifying multiple bands for detecting fecal contamination on the apples using the hyperspectral reflectance technique, four multispectral bands (450, 530, 685, and 735 nm) were identified as being the optimal bands to allow discrimination of fecal contaminated apple surfaces. Furthermore, a simple two-band ratio (e.g., 685 to 450 nm) was found to reduce the variation in normal apple surfaces while accentuating differences between contaminated and uncontaminated areas. This study indicates that multispectral fluorescence techniques can be used to effectively detect fecal contamination on apple surfaces. These results suggest that use of multispectral fluorescence techniques for detection of fecal contamination on apples in a commercial setting may be feasible. Detail of this study can be found in Kim, et al.[28]

Summary

Imaging spectroscopy, commonly called hyperspectral imaging, acquires images in which a spectral signature is associated with each spatial element or pixel, resulting in a 3-dimensional data cube of information, including 2 spatial dimensions and 1 spectral reflectance or fluorescence dimension. It combines the advantages of imaging and spectroscopic techniques. Textural and morphological information of the whole object or region is combined with color and compositional absorption (or in the case of fluorescence, emission) information at each pixel level. While hyperspectral imaging provides important spectral and spatial information, it does not have the capacity for rapid on-line, real-time data acquisition and processing. However, hyperspectral imaging data can be used for the selection of several spectral bands, which, when combined, subtracted, or mathematically manipulated, often provide important information for a variety of effective applications. The optimal bands and algorithms can then be implemented in multispectral imaging systems for rapid or real-time prediction or inspection of many food commodities for quality and safety.

References

1. J.S. Shenk, J.J Workman, Jr. and M.O. Westerhaus. In edited by D.A. Burns and E.W. Ciurczak. Handbook of Near-Infrared Analysis. 2nd Edition, Chapter 16. 419-474. Marcel Dekker, Inc. New York. (2001).
2. S.R. Delwiche, Y.R. Chen and W.R. Hruschka. Cereal Chemistry, **72**, 243 (1995).
3. S.R. Delwiche. J. of Cereal Science, **27**, 241 (1998).
4. Y.R. Chen and D.R. Massie. Trans. ASAE, **36**(3), 863 (1993).
5. Y. Liu and Y.R. Chen. Meat Science, **58**(4), 395 (2001).
6. B.P. Dey, Y.R. Chen, C. Hsieh and D.E. Chan. Poultry Science, **82,** 199 (2003).
7. Y.R. Chen, K. Chao, W.R. Hruschka and Y. Liu. In: (J.A.DeShazer and G.E.Meyer, Eds.) Optics in Agri. 1990-2000. SPIE, Critical Review, **80.** 140 (2001).
8. A. Davenel, C. Guizard, T. Labarre and F. Sevila**.** J. Agri. Eng. Res., **41**, 1 (1988).
9. G.E. Rehkugler and J.A. Throop. Trans. ASAE, **32,** 267 (1989).
10. T.P. McDonald and Y.R. Chen. Trans. ASAE, **34**(6), 2499 (1991).
11. N. Singh and M.J. Delwiche. Trans. ASAE, **37,** 1989 (1994).
12. W.R. Daley, R. Carey and C. Thompson. In Proceedings of SPIE, **2345**, 403 (1995).
13. K. Chao, Y.R. Chen, H. Early and B. Park. App. Eng, in Agri., **15**, 363 (1999).
14. A.Y. Muir, R.L. Porteous and R.L. Wastie. J. Agri. Eng. Res., **27**, 131 (1982).
15. S.K. Taylor and W.F. McCure. In Proc. of the 2nd International NIR Conference, Tsukuba, Japan, 393 (1989).
16. B. Park, Y.R. Chen and K. Chao. In: (Y.R. Chen, editor) Pathogen Detection and Remediation for Safe Eating. Proc. SPIE, **3544**, 156 (1998).
17. K. Chao, B. Park, Y.R. Chen, W.R. Hruschka and F.W. Wheaton. App. Eng. in Agri., **16,** 581 (2000).
18. K. Chao, Y.R. Chen, W. Hruschka and B. Park. App. Eng. in Agri., **17**(1), 99 (2000).
19. M.S. Kim, J.E. McMurtrey, C.L. Mulchi, C.S.T. Daughtry, E.W. Chappelle and Y.R. Chen. App. Optics, **40**(1), 157 (2001).
20. G. Shaw and D. Manolakis. IEEE Sign. Proc. Magazine, January 2002, 12 (2002).
21. M.S. Kim, Y.R. Chen and P.M. Mehl. Trans. ASAE, **44**(3), 721 (2001).
22. M.S. Kim, K. Chao, Y.R. Chen, D. Chan and P.M. Mehl. In: (Y.R. Chen and S.I. Tu, editors.) Photonic Detection and Intervention Technologies for Safe Food. Proc. SPIE, **4206,** 174 (2000).
23. D. Landgrebe. IEEE Signal Processing Magazine, January 2002, 17 (2002).
24. A. Talukder and D. Casasent. Opt. Eng.,37(03), 904 (1998).
25. R.O. Duda, P.E. Hart and D.G. Stork. Pattern Classification, 2nd edition, Wiley-Interscience, New York. (2001).
26. P.M. Mehl, Y.R. Chen and M.S. Kim. J. of Food Eng., (In press).
27. M.S. Kim, A.M. Lefcourt, K. Chao, Y.R. Chen, I. Kim and D. Chan. Trans. ASAE, **45**(6), 2027 (2002).
28. M.S. Kim, A.M. Lefcourt, Y.R. Chen, I. Kim, D.E. Chan and K. Chao. Trans. ASAE, **45**(6), 2039 (2002).